Light Metals 2013 *Edited by: Barry Sadler*
TMS (The Minerals, Metals & Materials Society), 2013

Light Metals 2013

ALUMINUM ALLOYS: FABRICATION, CHARACTERIZATION AND APPLICATIONS

Emerging Technology

SESSION CHAIR
Subodh Das
Phinix LLC
Lexington, KY USA

Light Metals 2013 *Edited by: Barry Sadler*
TMS (The Minerals, Metals & Materials Society), 2013

Transient microstructural thermomechanical fatigue and deformation characteristics under superimposed mechanical and thermal loading, in AlSi based automotive diesel pistons.

Roman Morgenstern[1], Scott Kenningley[1]
[1] Federal-Mogul Nürnberg GmbH, Nopitschstrasse 67, 90441 Nürnberg, Germany

Keywords: Aluminium, Thermomechanical, FEA, Superimposed, Fatigue

Abstract

Presently AlSi based alloys, consisting up to 12 element systems, are used in the manufacture of automotive pistons for light vehicle (LVD) and heavy (HD) duty diesel engines. The pistons combustion wall is subject to complex superimposed transient mechanical and thermal loading with peak operating temperature representing a homologous temperature range of 0.8-0.9 T_{hom}.
Using specialist superimposed thermomechanical bench test apparatus, 'engine like' TMF loading has been reproduced and a number of semi in-situ experiments have been carried out to evaluate key microstructure damage mechanisms. The evolution of microstructural damage at the interface between hard Si inclusions and the softer Al matrix has been documented using scanning electron microscopy. The deformation characteristics at the α-Al/ Si interface have been recreated using FEA techniques incorporating non-linear elasto-viscoplastic properties for the matrix material. Comparisons of bench test fatigue lives for transient superimposed high frequency and microstructural TMF loading, with fatigue lives from isothermal mechanical loading are also made.

Introduction

The use of AlSi based alloys provides a lightweight piston solution for the majority of today's automotive passenger car engine applications [1-3]. The present trends in engine development toward higher specific power output, lower fuel consumption and a requirement to adhere to increasingly tighter emissions controls results in higher thermal and mechanical loading on the automotive piston [1]. This is most evident in the development of light vehicle diesel (LVD) pistons, where peak temperatures reach ~420°C, representing a homologous temperature range of 0.8-0.9 T_{hom}. The continued use of the AlSi based alloys thus provides material scientists and engineers alike with the challenge of optimizing the materials for increased robustness at higher thermal and mechanical loads [1-4]. Currently piston alloy developments are looking to further optimize casting and secondary process parameters in synergy with alloying element content to provide microstructures capable of resisting present and future generation of in-cylinder engine load requirements [1, 2, 5].
To aid in the process development of new alloys research work is aimed at achieving a greater understanding of the micromechanical effects of superimposed 'engine like' thermal and mechanical loading on microcrack initiation and early growth. For AlSi based alloys micromechanical damage is dependent on a number of factors intrinsic to the alloy including casting defects, matrix strength, primary phase sizes, morphology and distributions. Previous research into the micromechanisms of damage at the α-Al/ Si interface has been predominantly concerned with monotonic tension/ compression and isothermal cyclic loading [6-11]. 'Engine like' thermomechanical fatigue (TMF) superimposed with high cycle mechanical fatigue (HCMF) loading or TMF/ HCMF has been previously reported [1, 5, 12, 13] for similar AlSi based alloys to that used in this study. Detailed modelling of the α-Al/ Si interface has been carried out at an atomistic level [14, 15] and on a microstructural level using FEA [16, 17].
This study provides an evaluation of the micromechanical fatigue damage observed at the primary α-Al/ Si matrix interface during semi in-situ isothermal HCMF and superimposed TMF/ HCMF bench testing. The macrostructural fatigue strength gained for 1E7 high cycles for superimposed TMF/ HCMF and isothermal HCMF loading are compared. Explanations of deformation under thermal loading, damage initiation mechanisms, and local stress discontinuity effects are supported with a 2D FEA of the experimental region of interest (ROI) under TMF loading.

Experimental and Material Details

Materials

The AlSi based alloy used for evaluation in the present study is the Federal-Mogul high durability piston material FM-B2, which primarily consists of Si: 12.0-14.5wt%, Cu: 3.7-5.2wt%, Ni: 1.7-3.2wt%, Mg: 0.5-1.5wt%, Fe: <0.7wt% and Al: balance. All the specimens used for fatigue testing in this study were extracted from the combustion bowl region of LVD piston castings after a standard T5 heat treatment process. The sample used for the semi in-situ evaluation was tested from the T5 heat treated state. This specimen was manufactured with a specially modified and polished gauge length to aid in observations using light optical (LOM) and scanning electron (SEM) microscopy at stepwise intervals during testing. The fatigue test specimens for isothermal HCMF and superimposed TMF/ HCMF were all thermally over aged for 200hrs at 350°C prior to testing.

Apparatus

The isothermal HCMF and superimposed TMF/ HCMF tests were carried using specially adapted bench test apparatus housed in the Federal-Mogul technical centre in Nürnberg, Germany. The specimen heating and cooling arrangement uses inductive heating with a cooled specimen grip system. This system has been optimized to minimize thermal gradients across the sample and ensure a triangular wave temperature vs time plot with heating/cooling rates typical of those measured in the combustion bowl region of the component during variable load engine operation. In this study, the thermal cycle was operated in the range T_{min} 200°C to T_{max} 440°C with a ΔT of 10K/s. No thermal constraint parameter was imposed on the specimen during thermal cycling; i.e. no mechanical strain is imposed with a change in temperature, such that a mean stress of zero is maintained during superimposed testing. The superposition of HCMF loading was done with a fully reversed sinusoidal load signal (R=-1) at a load

frequency of 70Hz. The isothermal HCMF tests were run using the same system as for the TMF/ HCMF testing.

Semi in-situ HCMF and TMF/ HCMF test cycle design

The semi in-situ α-Al/ Si interface experiment began with intermittent removal and imaging of the specially manufactured test specimen over a period of 1E7 HCMF cycles run isothermally at a temperature of 350°C with a constant stress amplitude of 30MPa. After the completion of the HCMF cycles a further 3500 superimposed TMF/ HCMF cycles were run with the same HCMF stress amplitude of 30MPa maintained throughout the test.

HCMF and superimposed TMF/ HCMF testing

The HCMF specimens were tested under isothermal conditions at 350°C and 440°C. The TMF/ HCMF specimens operated using the thermal cycle described in the apparatus section. In order to provide a comparison of the equivalent fatigue strength at 1E7 mechanical high cycles, testing was done at multiple mechanical stress amplitudes and with sufficient sample batch sizes to provide statistically useful 'development' comparisons. The lifetime or S-N curve results were fitted using a least squares approach on a first order power law or Basquin type equation. From this analysis the mean fatigue strength and standard deviation were derived.

Microstructure Evaluation

Characterization of the microstructure and imaging of the interfacial region between the primary Si phases and α-Al matrix was done using a Carl Zeiss EVO MA15 SEM with an LaB6 cathode in secondary electron mode. Images were taken using a 5kV acceleration voltage and beam I-probe current of 10pA at a working distance of 14mm.

Finite Element Analysis (FEA)

An embedded micromechanical finite element model (FEM) for the microstructural ROI containing two primary Si particles was developed for analysis. The geometry was created using a simple image thresholding and geometrical de-featuring approach. The geometry was then meshed using second order 2D triangular plane strain elements. The material model for the α-Al matrix was a non-linear temperature dependent elasto-viscoplastic (EVP) model. The primary Si particles were modeled as a single feature with temperature dependent elastic properties. The boundary embedding zone surrounding the α-Al matrix was modeled with the EVP properties for the AlSi based alloy. In this study, the thermal cycle was modeled to assess the uncoupled TMF effects at the interface. Four cycles were modeled to achieve near stable σε hysteresis.

Results and Discussion

Microstructural features

The pre-test microstructural ROI is shown in Figure 1, with the dendritic α-Al matrix structure embedded with interdendritic primary Si, eutectic Si and various intermetallic phases. The morphology and size of the primary Si particles is typical of the gravity die cast (GDC) alloy.

Isothermal HCMF effects on the microstructure

Figure 2(a-b) shows the evolution of the microstructure over 1E7 HCMF cycles at 350°C. During the HCMF testing the α-Al/ Si interface shows no visible evidence of damage. The most notable feature change during HCMF testing is the precipitation of the age hardening secondary phases, shown initially in Figure 2a at 1.5E6 HCMF cycles, and then after their continued coarsening to the end of the HCMF test phase, Figure 2b, at 1.0E7 fatigue cycles.

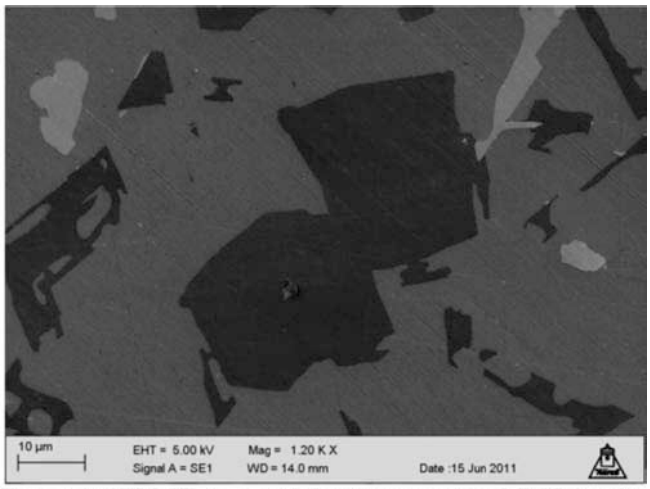

Figure 1: SEM SE image of the microstructural ROI for the AlSi based alloy in the pre- semi in-situ test condition. Centrally focused are two primary Si particles.

Superimposed TMF/ HCMF effects on the microstructure

Figure 2(c-f) shows the morphology of the microstructure when subjected to the superimposed TMF/ HCMF loading. The first imaging interval, shown in Figure 2c, was made after the completion of 50 thermal cycles. In comparing Figure 2c with Figure 2b, a large volume fraction of the secondary phase precipitates have been taken back into solution while at the primary phase interfaces there are the initial signs of α-Al matrix plasticity. The α-Al matrix plasticity continues to develop during subsequent thermal cycles with images being taken intermittently after 500, 2000 and 3500 TMF/ HCMF cycles, shown in Figure 2(d-f) respectively. After 500 cycles the local plastic zones originating at the primary phase interfaces have already grown in size and coalesced such that the entire inter-particle region of the α-Al matrix appears plastically deformed. After 2000 cycles the first signs of interfacial debonding at the α-Al/ Si interface are apparent. The continued microstructural damage evolution after 3500 thermal cycles shows the interfacial zone to have extensive damage with substantial localized debonding, void nucleation and microcrack initiation evident. Magnified examples of the interfacial debonding are shown in Figure 3, while examples of interfacial void and microcracks are highlighted close to the fracture surface from a TMF/ HCMF specimen failure in Figure 8.

Deformation mechanisms at the α-Al / Si interface

For AlSi based highly alloyed materials, subject to temperature exposure, internal stresses will exist regardless of external constraint due to the differential mismatch in thermal and

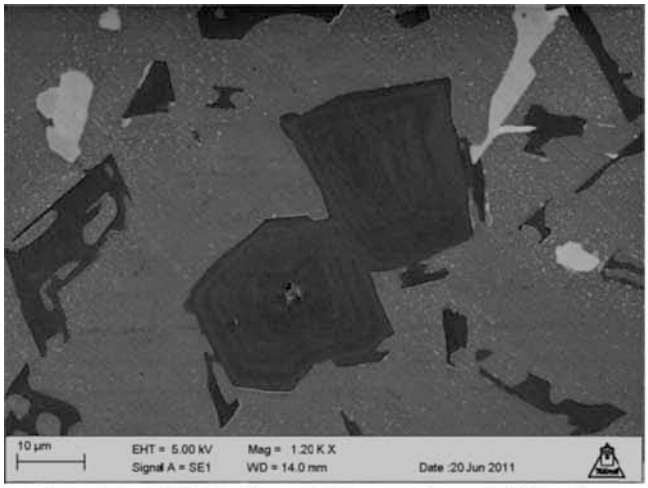

(a) After 1.5E6 isothermal fatigue cycles at 350°C with a stress amplitude of 30MPa.

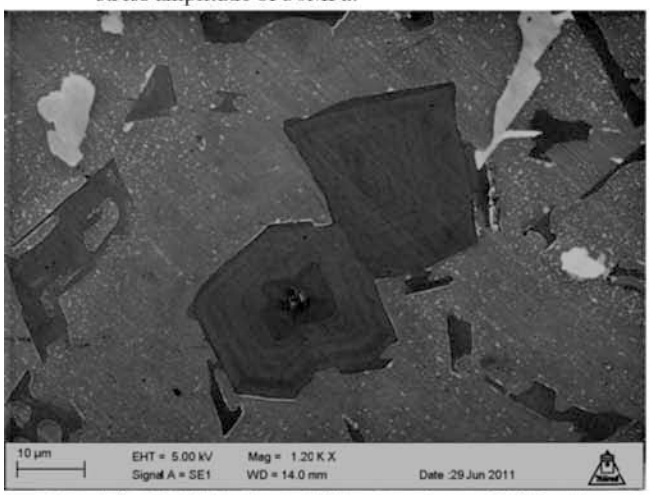

(b) After 1.0E7 isothermal fatigue cycles at 350°C with a stress amplitude of 30MPa.

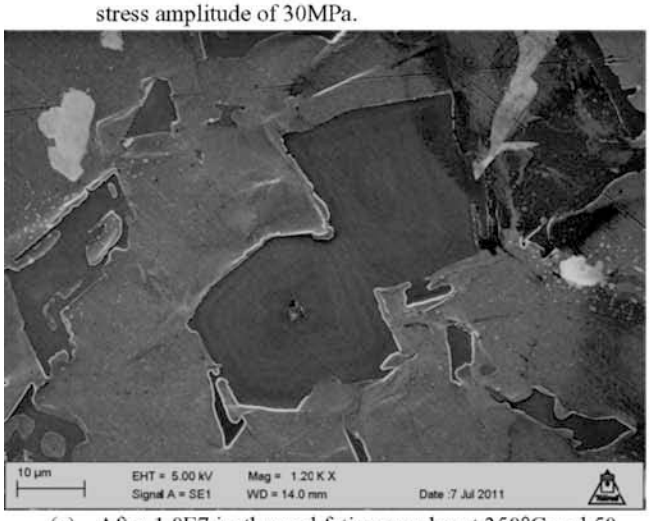

(c) After 1.0E7 isothermal fatigue cycles at 350°C and 50 superimposed TMF/ HCMF cycles. A thermal cycle running between T_{min} 200°C – T_{max} 440°C with a high cycle stress amplitude of 30MPa.

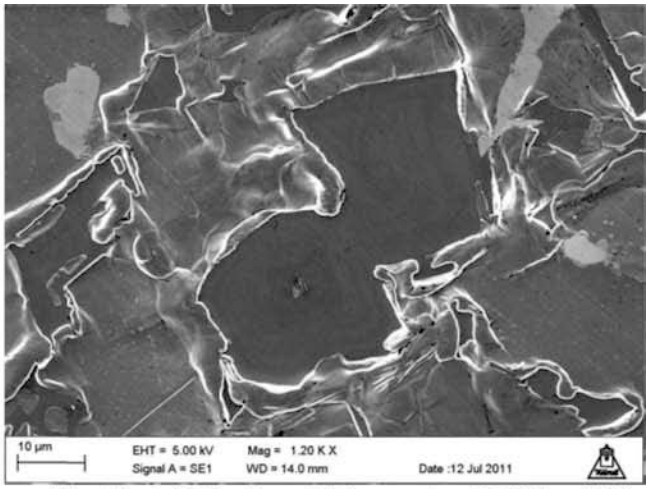

(d) After 1.0E7 isothermal fatigue cycles at 350°C and 500 superimposed TMF/ HCMF cycles (as described in (c)).

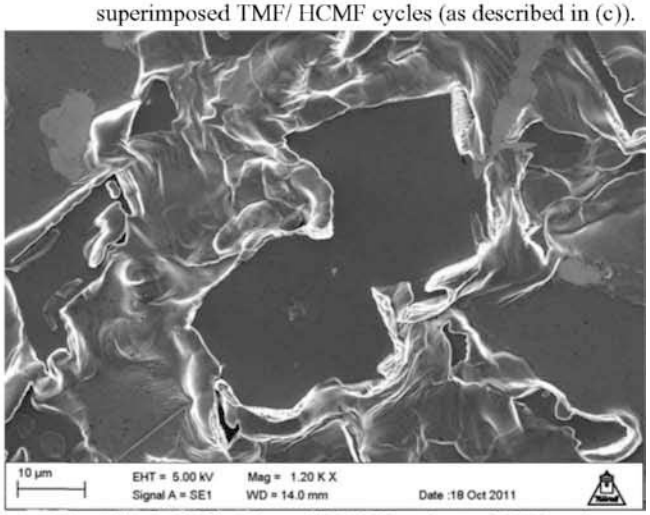

(e) After 1.0E7 isothermal HCMF cycles at 350°C and 2000 superimposed TMF/ HCMF cycles (as per (c)).

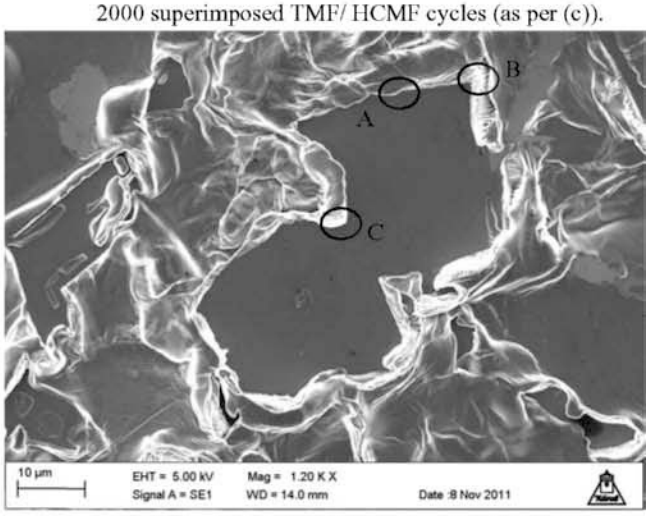

(f) After 1.0E7 isothermal HCMF cycles at 350°C and 3500 superimposed TMF/ HCMF cycles (as per (c)).

Figure 2(a-f): SEM SE images of the AlSi based alloys ROI taken during the semi in-situ HCMF and superimposed TMF/ HCMF experiments.

mechanical properties between the α-Al matrix and the reinforcing primary phases. Internal residual stresses in the interfacial regions will therefore be present from the initial cooling from the gravity die casting (GDC) manufacturing process. Any internal residual stresses remaining after the T5 heat treatment which follows the casting process will be quickly removed when the component is heated to temperatures above 300°C through relaxation/ recovery mechanisms. For the isothermal HCMF testing with a fully reversed (R=-1) load cycle, thermal stress levels are not thought to be significant at test temperatures of 350°C and 440°C and the microstructure is assumed to be exposed to cyclic deformation alone from the driven mechanical sinusoidal load.

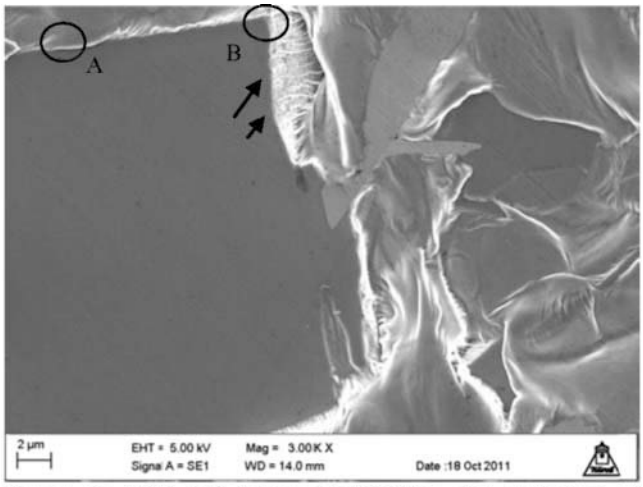

Figure 3: SEM SE image highlighting the evolution of interfacial debonding after 1.0E7 isothermal fully reversed (R=-1) fatigue cycles (T=350°C Δσ/2=30MPa) and 2000 superimposed TMF/ HCMF cycles. A thermal cycle running between T_{min} 200°C – T_{max} 440°C with a fully reversed high cycle stress amplitude of 30MPa.

When subjected to thermal cycling, the continual changes in temperature have the effect of regenerating the internal microstructural σε tensor each cycle. The varying thermally induced σε tensor acts as a mean onto which the high frequency reversed mechanical load signal is superimposed.

Using a simple 2D geometrical FE model of the microstructural ROI, as shown in Figure 4, analysis has been done to help explain the deformation characteristics during thermal cycling. While in reality, the α-Al/ Si interface will be subject to a tri-axial state of stress, a simple bi-axial explanation is considered reasonable in this work based on the created 2D geometry. The analytical predictions of the local σ-T and $\varepsilon_{mechancial}$-T relationships, taken from the analysis of the fourth thermal cycle are graphically shown, for three positions on the primary Si boundary A, B and C from Figure 4, in Figure 5(A-B) and Figure 6(A-B) for directions radial and parallel to the Si interface respectively. At the planar interface (A) the α-Al matrix σ_{radial} is tensile during heating as it tries to expand further and faster than the Si interface. During the cooling segment of the thermal cycle, the faster α-Al matrix contraction results in a compressive σ_{radial} effect on the interface, as shown in Figure 5(A&B). Figure 6(A&B) shows that the subsequent effects on the $\sigma_{parallel}$ to the interface are opposite in nature, being compressive during heating as the α-Al matrix is squeezed and tries to expand radially away from the Si interface and then tensile during cooling as the contraction is restricted by the Si and the material tries to *press* across the interface. If the results of the planar surface position (A) are compared with the tensors for the cubic corner position (B), it can be seen that the trends during heating and cooling are similar, but the magnitudes of strain have more than doubled at the high temperature point of the cycle, as shown in Figure 5(A) and Figure 6(A). The extent to which the microstructure is able to accommodate the higher load at the cubic corner location, through recovery and damage mechanisms, is a key issue in the initiation of interfacial debonding, void growth and microcracking. Assessment of the tensors at the re-entrant position (location (C)) show that the stress and strain tensors shift in phase with temperature. This phase shift is a function of the local constraint conditions imposed by the Si, further outlining the complexity of the local deformation characteristics.

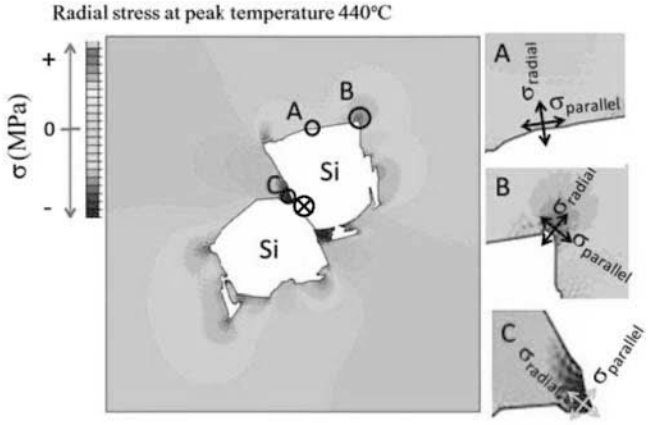

Figure 4: 2D FE model representing the AlSi based alloy microstructure ROI. The plot represents the radial stress at 440°C referenced from the model origin ⊗ using a cylindrical co-ordinate system. The inset images A, B and C represent significant points of interest at the Al/ Si interface with σ_{radial} and $\sigma_{parallel}$ highlighted and extracted for graphical representation using localized rectangular co-ordinate systems.

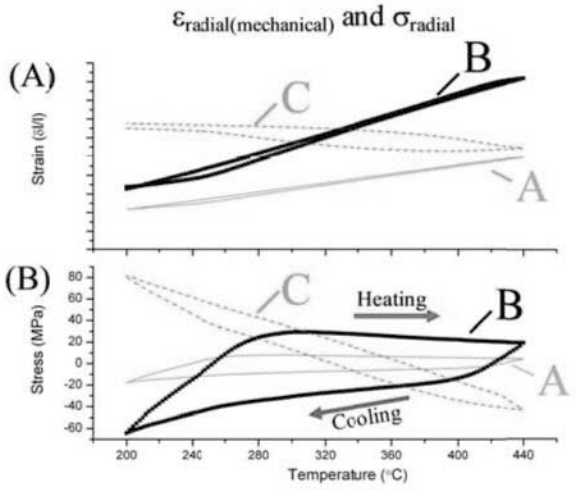

Figure 5(A-B): Hysteresis of (A) $\varepsilon_{radial(mechanical)}$ against temperature and (B) σ_{radial} against temperature. Data extracted from the fourth thermal cycle of a FEA running

between T_{min} 200°C – T_{max} 440°C. The highlighted curves A, B and C represent the specific ROI identified in Figure 4. The heating segment of the thermal cycle is represented in all cases by the upper bounding line between turning points of the hysteresis.

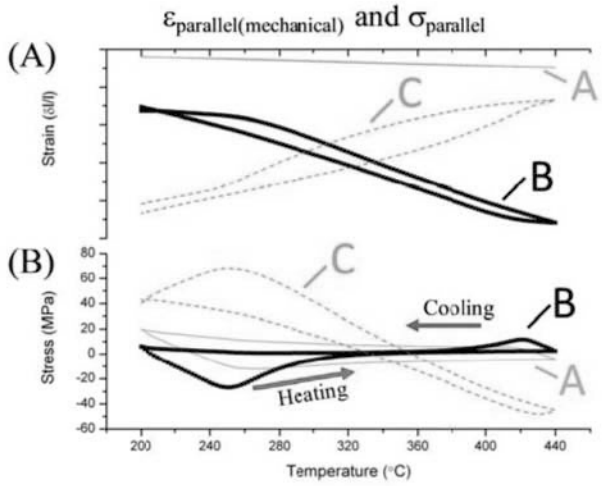

Figure 6(A-B): Hysteresis of (A) $\varepsilon_{parallel(mechanical)}$ against temperature and (B) $\sigma_{parallel}$ against temperature. Data extracted from the fourth thermal cycle of an FEA running between T_{min} 200°C – T_{max} 440°C. The highlighted curves A, B and C represent the specific ROI identified in Figure 4. The heating segment of the thermal cycle is represented in all cases by the lower bounding line between turning points of the hysteresis.

Lifetime characteristics of HCMF and TMF/ HCMF loading

The comparison of stress based fatigue strength at 1E7 equivalent high cycles is graphically shown in Figure 7 for isothermal HCMF testing at 350°C, 440°C and for the TMF/ HCMF testing. The result shows the superimposed TMF/ HCMF loading (consisting of an unconstrained thermal cycle) has an 8% higher and 6% lower mean 1E7 high cycle fatigue strength than the isothermal HCMF results for 440°C and 350°C respectively.

Damage Mechanisms

During fully reversed cyclic fatigue loading, AlSi based piston alloys spend the majority of their total fatigue life in the micro crack incubation stage. The evolution from microcracks to microstructurally small cracks to physically small and then finally to long fatigue cracks occur at a high rate. At high temperatures the long fatigue cracks tend to run along brittle primary alloy phase boundaries with shear across the intervening regions of ductile matrix to final fracture. At lower temperatures the long fatigue crack incident on primary Si can often induce particle fracture.

The initiation sites for microcracks are preferentially at stress concentrations. For AlSi based alloys, the stress discontinuities are provided by primary silicon, eutectic Si, intermetallic phases, casting defects (pores and oxides). The presence of pores and oxides in highly stressed regions are generally accepted as being most detrimental to fatigue, reducing lifetimes by in excess of an order of magnitude when ideally positioned and of sufficient size [8].

This study is concerned with the micromechanisms of failure at the α-Al/ Si interface. In the absence of casting defects, failure originating from decohesion and microcrack growth at the interface between the primary Si phase and the α-Al matrix is normal [10, 18, 19].

The semi in-situ tests in this study have shown that interfacial stress concentrations, occurring under superimposed cyclic TMF/ HCMF loading induced high levels of microplasticity around the cubic primary silicon pair, as shown in Figure 2f, leading to localized interfacial debonding and micro void nucleation. The events leading to debonding and void nucleation are a result of the complex interaction of dislocations, vacancies and local chemistry at the interface influenced by the local σε and temperature conditions. The initiation sites for decohesion have been shown to be sensitive to the stress concentrations provided by the corners of

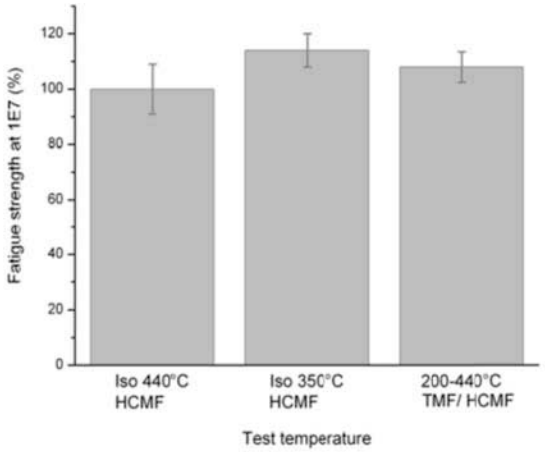

Figure 7: A graphical representation of the calculated fatigue strength at 1E7 cycles for isothermal HCMF testing at 350°C and 440°C compared with the superimposed TMF/ HCMF results for the tests run with zero thermal constraint. The error bars represent the standard deviation from the statistical analysis.

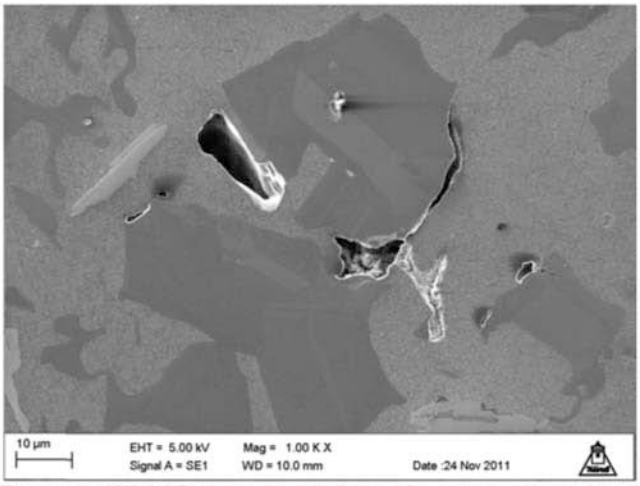

Figure 8: SEM SE image highlighting the extent of interfacial micromechanical damage at the Al/ Si interface taken from particles close to a fracture surface of a superimposed TMF/ HCMF test specimen with failure occurring in excess of 1E7 high cycles.

the cubic shape of the primary Si particles and by the re-entrant angle created between the two Si particles, as shown in Figure 2f and Figure 3. Regions of interfacial debonding and void growth are essentially stress raising discontinuities acting as initiation sites for microcracks. The propagation of these microcracks is sensitive to the local micro-geometry with not all the cracks necessarily leading to long fatigue cracks [6]. Within the microstructure it is expected that there are many microcrack initiation events occurring at highly stressed locations. As these microcracks propagate, they may coalesce or link to form firstly a microstructurally or physically small crack which then goes onto to evolve into a long fatigue crack eventually leading to final fracture. As microstructurally small and long cracks propagate through the interdendritic α-Al matrix regions, they come into contact with Si particles and intermetallics which generally have the effect of arresting the crack growth rate and deflecting the cracks around them incurring debonding along their interfaces. If the stress concentration is high enough at the interface, Si particle fracture is possible affecting long and microcrack growth characteristics. During thermal cycling, it is more likely that Si particle fracture would occur in the low temperature regime.

Conclusions

It is generally well accepted that in the absence of intrinsic casting flaws the fatigue of AlSi based piston alloys can be dominated by Si particle morphology with initiation more prevalent along the interfaces of larger primary Si cuboids in regions of favorably stressed micro-geometry. The local heterogeneity in highly alloyed AlSi microstructures makes it difficult to quantify the effect of any single microstructural feature on fatigue life. In this study micromechanical damage under 'engine like' superimposed TMF/ HCMF loading has been identified and discussed with respect to a local microstructural ROI.

The semi in-situ tests showed how superimposed TMF/ HCMF loading can increase the micromechanical fatigue damage in comparison to the isothermal HCMF loading. This is primarily a function of the repetitive thermal $\sigma\varepsilon$ tensor induced during heating and cooling. This thermal $\sigma\varepsilon$ tensor is induced due to the mismatch in thermal expansion between the Si phases and α-Al matrix in the alloy microstructure.

The FEA model predictions under thermal cycling conditions showed the heterogeneous state of stress around two cubic clustered primary Si particles. The locations of the high load discontinuities show some correlation to the regions of increased interfacial damage.

The TMF/ HCMF loading, featuring an unconstrained triangular thermal cycle running between T_{min} 200°C and T_{max} 440°C, provided mean fatigue strength results between the values gained for isothermal HCMF test results at 350°C and 440°C.

Acknowledgements

With thanks to the Federal-Mogul Technology team, especially to Robert Willard, Neil Wardrop and Georg Hopp.

References

1. Kenningley, S. and R. Morgenstern, *Thermal and Mechanical Loading in the Combustion Bowl Region of Light Vehicle Diesel AlSiCuNiMg Pistons; Reviewed with Emphasis on Advanced Finite Element Analysis and Instrumented Engine Testing Techniques.* SAE Technical Paper 2012-01-1330, 2012.
2. Reichstein, S., P. Konrad, and S. Kenningley, *Microstructure modification of piston materials for high stress and temperature conditions.* Aachener Kolloquium Fahrzeug- und Motorentechnik 2007, 2007.
3. Reichstein, S., et al., *High-Performance Cast Aluminum Pistons for Highly Efficient Diesel Engines.* SAE Technical Paper 2007-01-1438, 2007.
4. Barnes, S. and K. Lades, *The Evolution of Aluminium Based Piston Alloys for Direct Injection Diesel Engines.* SAE Technical Paper 2002-01-0493, 2002.
5. Humbertjean, A. and T. Beck, *Effect of the casting process on microstructure and lifetime of the Al-piston-alloy AlSi12Cu4Ni3 under thermo-mechanical fatigue with superimposed high-cycle fatigue loading.* International Journal of Fatigue, 2011.
6. McDowell, D.L., et al., *Microstructure-based fatigue modeling of cast A356-T6 alloy.* Engineering Fracture Mechanics, 2003. **70**(1): p. 49-80.
7. Jordon, J.B., et al., *Microstructural Inclusion Influence on Fatigue of a Cast A356 Aluminum Alloy.* Metallurgical and Materials Transactions a-Physical Metallurgy and Materials Science, 2010. **41A**(2): p. 356-363.
8. Wang, Q.G., D. Apelian, and D.A. Lados, *Fatigue behavior of A356-T6 aluminum cast alloys. Part I. Effect of casting defects.* Journal of Light Metals, 2001. **1**(1): p. 73-84.
9. Wang, Q.G., D. Apelian, and D.A. Lados, *Fatigue behavior of A356/357 aluminum cast alloys. Part II – Effect of microstructural constituents.* Journal of Light Metals, 2001. **1**(1): p. 85-97.
10. Mbuya, T.O., et al., *Micromechanisms of fatigue crack growth in cast aluminium piston alloys.* International Journal of Fatigue, 2012. **42**(0): p. 227-237.
11. Han, S.-W., S. Kumai, and A. Sato, *Effects of solidification structure on short fatigue crack growth in Al–7%Si–0.4%Mg alloy castings.* Materials Science and Engineering: A, 2002. **332**(1–2): p. 56-63.
12. Beck, T., et al., *Damage mechanisms of cast Al-Si-Mg alloys under superimposed thermal-mechanical fatigue and high-cycle fatigue loading.* Materials Science and Engineering a-Structural Materials Properties Microstructure and Processing, 2007. **468**: p. 184-192.
13. Beck, T., I. Henne, and D. Loehe, *Lifetime of cast AlSi6Cu4 under superimposed thermal-mechanical fatigue and high-cycle fatigue loading.* Materials Science and Engineering a-Structural Materials Properties Microstructure and Processing, 2008. **483-84**: p. 382-386.
14. Gall, K., et al., *Atomistic simulations on the tensile debonding of an aluminum–silicon interface.* Journal of the Mechanics and Physics of Solids, 2000. **48**(10): p. 2183-2212.
15. Ward, D.K., W.A. Curtin, and Y. Qi, *Aluminum–silicon interfaces and nanocomposites: A molecular dynamics study.* Composites Science and Technology, 2006. **66**(9): p. 1151-1161.
16. Gall, K., et al., *Finite element analysis of the stress distributions near damaged Si particle clusters in cast Al–Si alloys.* Mechanics of Materials, 2000. **32**(5): p. 277-301.

17. Fan, J., et al., *Cyclic plasticity at pores and inclusions in cast Al–Si alloys.* Engineering Fracture Mechanics, 2003. **70**(10): p. 1281-1302.
18. Moffat, A.J., *Micromechanistic analysis of fatigue in aluminium silicon casting alloys*, University of Southampton: Southampton, 2007. p. 296.
19. Moffat, A.J., et al., *The effect of silicon content on long crack fatigue behaviour of aluminium–silicon piston alloys at elevated temperature.* International Journal of Fatigue, 2005. **27**(10–12): p. 1564-1570.